Final Technical Report for USGS/NEHRP #05HQGR0053 (UofO #238801)

Project Title: Quantifying Cascadia's Locked and Transition Zones Using Central Oregon Coastal Leveling and Tidal data

PIs: Ray Weldon & David Schmidt, University of Oregon, (contact: ray@uoregon.edu or 541-346-4584) Project Period: January 1, 2006 – December 31, 2007

SUMMARY

This project was to re-analyze existing leveling and tidal records, generate new data in selected areas and to model the data to determine the distribution of locking on the Cascadia Subduction Zone offshore Oregon. Increasingly the locking associated with the Cascadia Subduction zone is modeled with ever-improving horizontal GPS data; however, traditional vertical measurements of strain accumulation from tide gauges and leveling provide a denser and possibly more sensitive probe of strain accumulation on the Subduction Zone. This report is divided into two portions; part one is a re-analysis and modeling of existing easily accessible NGS and NOAA data, that is being published in the Journal of Geophysical Research (Burgette et al. in press). Part two is a preliminary presentation of our efforts to establish new tide gauges and leveling lines to fill in critical gaps in the regional coverage. This grant provided major support for Graduate Student Reed Burgette, partial support for Graduate Students Beth Wisely, Sean Bemis and Haiying Gao, and 6 Undergraduates (esp. Sarah Hunt and Tyler Claycomb).

Part 1: Re-analysis and modeling of existing NGS and NOAA data

While a number of authors have attempted to draw inferences from the existing NGS and NOAA data, it is clear that the data contain numerous systematic errors and blunders that have limited its usefulness. We believe we have overcome these problems by carefully testing all of the data for consistency by comparing individual benchmark stabilities, tilts from multiply repeated leveling lines and consistency between tidal and leveling derived tilt rates. In addition, we have extended the easily available tide gauge data with previously unanalyzed archive data and more robustly attached the tilts to an absolute (sea level based) reference frame. A summary of sea level results is included in Table 1 and Figure 1.

Table 1. Observed and Adjusted Relative Sea Level (RSL) Rates

Site or difference	Observed RSL rate (mm/yr)	Autocorrelation parameter (ρ)	S.E. from Lin. Reg. (mm/yr)	S.E. from Hildreth-Lu (σ_{ts}) (mm/yr)	Adjusted RSL rate (mm/yr)	Residual (v) (mm/yr)	v/σ_{ts} (%)	Adjusted S.E. (σ_{tg}) (mm/yr)
CC	-0.71	0.48	0.11	0.18	-0.54	0.17	93	0.08
PO	0.04	0.52	0.32	0.62	-0.31	-0.35	-56	0.10
Ch	0.66	0.49	0.26	0.45	0.29	-0.38	-84	0.09
SB	1.39	0.46	0.23	0.38	1.22	-0.17	-45	0.08
Ga	0.85	0.05	0.31	0.38	0.88	0.04	9	0.09
As	0.06	0.32	0.09	0.13	0.04	-0.02	-18	0.07
CC-PO	-0.05	0.48	0.13	0.23	-0.23	-0.19	-82	
CC-Ch	-0.79	0.32	0.11	0.15	-0.82	-0.03	-22	
CC-SB	-1.58	0.27	0.12	0.17	-1.76	-0.17	-104	
CC-Ga	-1.27	0.11	0.29	0.34	-1.42	-0.16	-45	
CC-As	-0.67	0.27	0.08	0.11	-0.58	0.09	84	
PO-Ch	-0.53	0.45	0.12	0.20	-0.59	-0.07	-34	
PO-SB	-1.55	0.43	0.14	0.24	-1.52	0.03	11	
PO-Ga	-1.13	0.11	0.27	0.32	-1.19	-0.06	-18	
PO-As	-0.26	0.38	0.19	0.31	-0.35	-0.08	-27	
Ch-SB	-0.96	0.48	0.07	0.12	-0.93	0.03	21	
Ch-Ga	-0.79	0.15	0.20	0.25	-0.60	0.20	77	
Ch-As	0.44	0.32	0.12	0.18	0.25	-0.19	-108	
SB-Ga	0.30	0.10	0.12	0.14	0.33	0.03	21	
SB-As	1.26	0.41	0.09	0.13	1.18	-0.08	-58	
Ga-As	0.77	0.17	0.13	0.18	0.84	0.07	42	

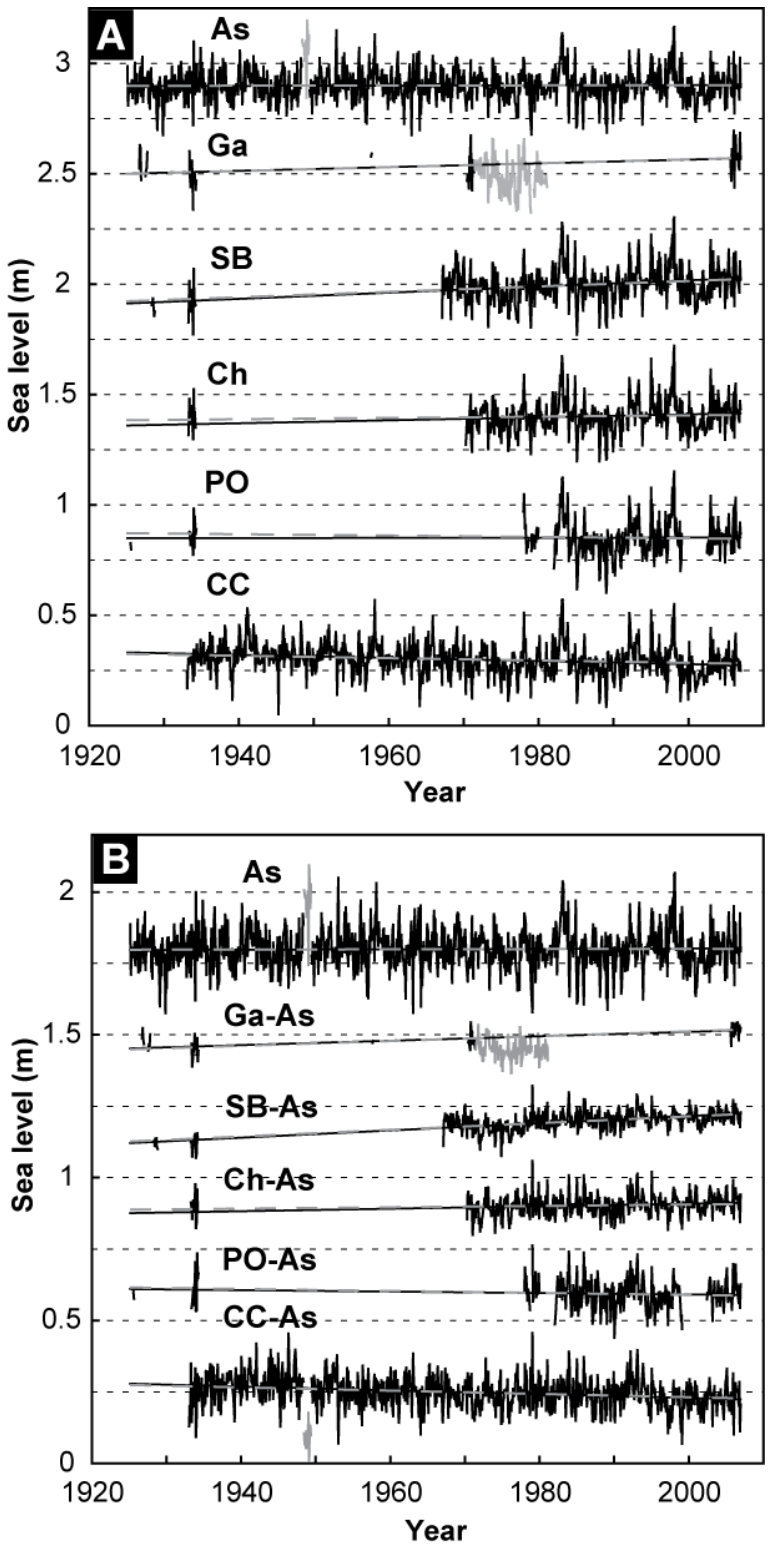

Figure 1. Sea level time series collected by National Ocean Service for Oregon portion of Cascadia. (a) Time series for each gauge, corrected for instabilities of primary benchmarks, with site-specific mean seasonal cycle removed, and river effect removed for Astoria. See Figure 5 for example of processing. We have extended the records of

the four central tide gauges with archived pre-1960 data to better constrain the relative sea level trends over the last century and all records are updated through 2006. Gray data from Astoria and Garibaldi are excluded from the analysis as explained in the text. Straight black lines are linear regression fits, and the dashed gray lines have the slopes determined from the least-squares adjustment, which incorporates the rates from the more precise differenced time series. Note that the adjustment only modifies the trends slightly, but this increases the confidence in the values of the trends.

(b) Example of differenced time series, using Astoria. Top As time series is same data shown in Figure 7a- note the change in scale. Below are the differences of Astoria from each of the other sites, arrayed north to south. Note that the scatter around the regression lines is reduced compared to the original time series, as shared ocean noise is removed. The scatter around the trend lines increases as the sites become more widely separated (moving down in the figure).

A key aspect in getting the sea level rise right has been to look at tidal benchmark stability; we found that most benchmarks are unstable and that key (primary) benchmarks at NOAA's tide gauge sites have settled or risen through time. A particularly serious example is shown in Figure 3, but most records required at least minor adjustments.

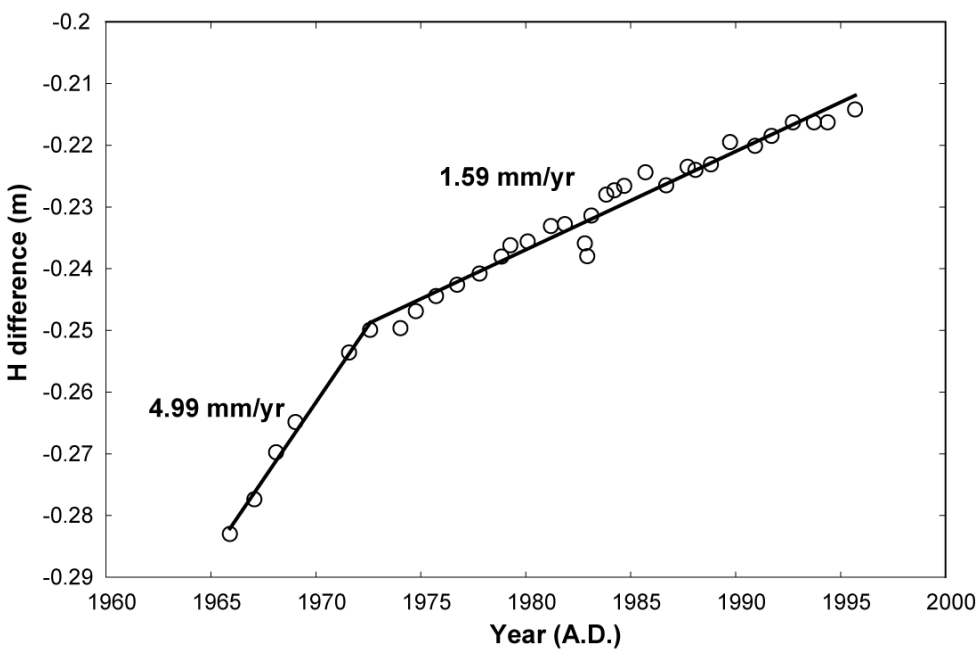

Figure 2. Time series of elevation difference of South Beach primary benchmarks from local tidal leveling. Elevation difference calculated as height of benchmark C 590 minus the height of benchmark A 590. Positive slope indicates that A 590, which lies on young sediment, was settling relative to C 590. Differencing these benchmarks from others in the tidal loop shows that A 590 subsided relative to its neighbors, while C 590 shows little relative motion. Leveling ties to the benchmarks on the Highway 101 bridge over the Yaquina River, which has footings on bedrock, indicate that C 590 is stable with respect to benchmark Y 1, which has been releveled in the NGS regional campaigns and

appears stable relative to other monuments in the Newport area. We correct the 2/1967 to 8/1996 portion of the South Beach tidal time series when A 590 was the primary benchmark using the slopes from the two regression lines shown fit to the data above.

The second key to recognizing errors in both the leveling and tidal records has been to compare the tilts (relative uplift rates) between tide gauges, determined by both leveling and relative sea level changes. This was particularly important for what we interpret to be a serious systematic error with the 1987/88 leveling epoch between Charleston and South Beach.

Table 2. Comparison of Tidal and Leveling Relative Uplift Rates

Coastal segment	D (km)	Leveling difference (mm/yr)			Tidal difference (mm/yr)			Leveling - Tidal (mm/yr)		
CC-PO	160	-0.04	±	0.33	0.23	±	0.19	-0.28	±	0.38
PO-Ch	123	-0.08	±	0.28	0.59	±	0.26	-0.67	±	0.38
Ch-SB	174	3.29	±	0.36	0.93	±	0.38	2.36	±	0.52
Ch-SB[a]		1.62	±	0.36				0.69	±	0.52
SB-Ga	144	0.04	±	0.36	-0.33	±	0.44	0.38	±	0.57
Ga-As	115	-0.28	±	0.32	-0.84	±	0.44	0.57	±	0.54

[a] Ch-SB leveling relative uplift rate after correction of systematic error as discussed in text

The results of our analysis are shown in Figure 3, which plots all of the stable benchmarks for which we were able to determine the uplift rate. The uplift rate varies systematically up and down the coast of Oregon and cannot be simply due to the distance from the subduction interface (white lines) as has previously been inferred by many authors. To model this data we grouped regions with significant east-west variation (boxes on Figure 3) and generated trench perpendicular profiles that were fit with simple elastic dislocation models. The model parameters were interpolated in between using the north south data between boxes to control the interpolation parameters, to determine the best fit to the entire data set. Residuals obtained by subtracting the model from the data generally reduced the range by an order of magnitude.

The distribution of locking, shown with lines on the downdip extent of complete locking (the region between the trench and the downdip extent of complete locking is called the “locked zone”) and the downdip extent of fractional locking (called the “transition zone”) is shown on Figures 4 and 5. Figure 4 compares the distribution to obvious geological features in the fore arc, such as the location of fore arc basins and the lateral extent of Siletzia, a large accreted oceanic plateau. Figure 5 compares our results to those of other workers. In general our model matches earlier models based on vertical strain data but is somewhat more sinuous, reflecting our greater resolution compared to past work. More recent models that are based mainly on the horizontal motion of GPS sites appear to suggest much wider transition zones.

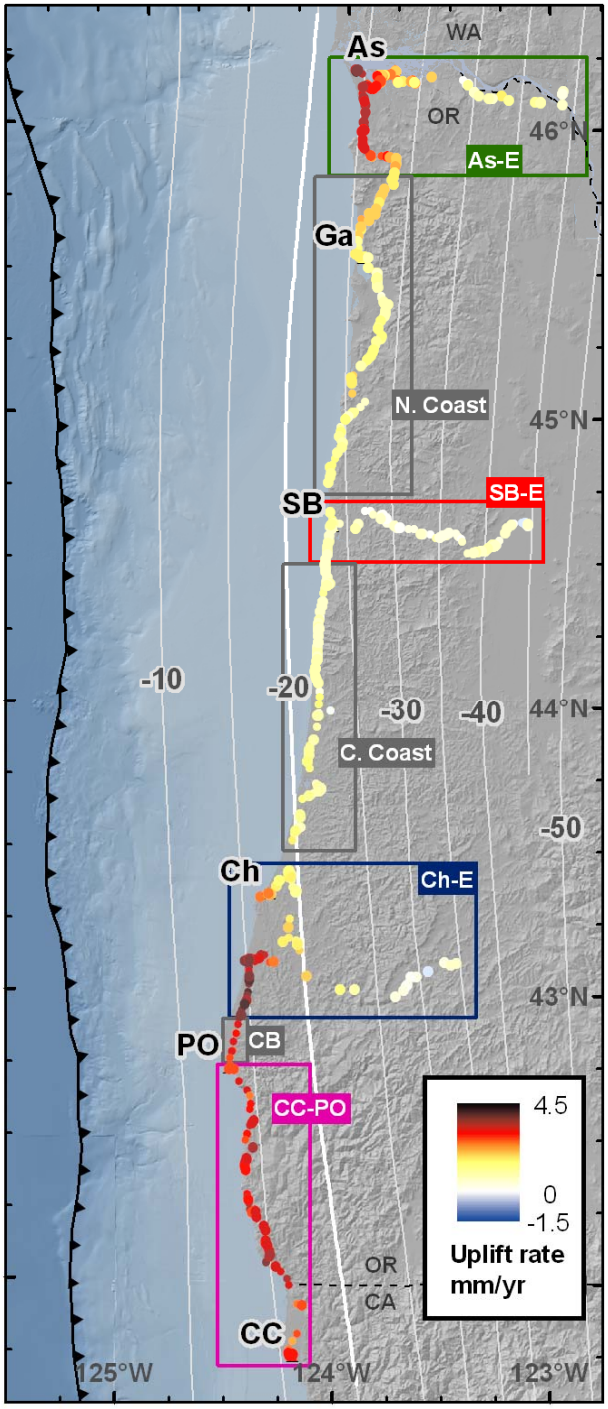

Figure 3. Uplift rates for benchmarks along releveled routes in western Oregon and northernmost California are colored by the scale in the lower right. In the central part of the map, uplift rates vary systematically, with the greatest values occurring above up-dip portions of the slab and declining inland. The southernmost section (CC-PO) has lower uplift rates despite being slightly updip relative to the central area. Note the contour-parallel gradient in uplift rates from SB north to As. The line east from As shows a similar downdip decrease in uplift rate, although shifted downdip relative to the slab compared to the central area.

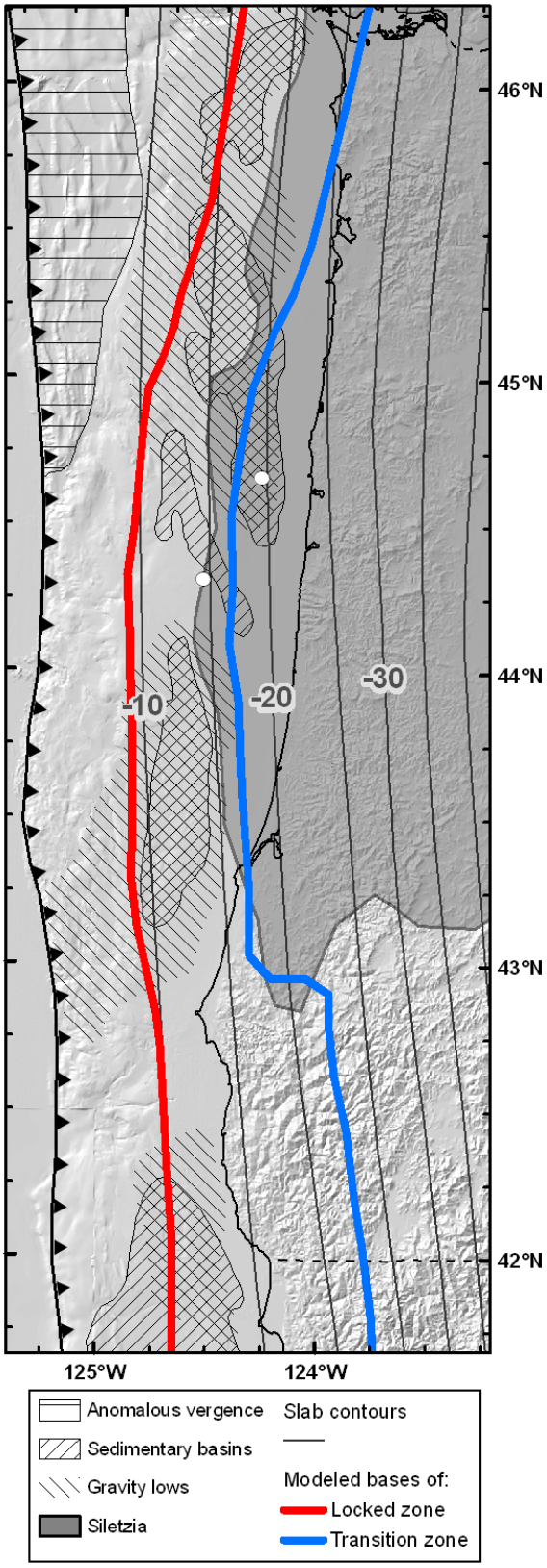

Figure 4. Modeled extents of the locked and transition zones, compared to major geologic features of the Cascadia forearc. The subsurface extent of the mafic Siletzia block is generalized from local and regional studies of the forearc [Wells et al., 1998; Parsons et al., 1999; McNeill et al., 2000; Blakely et al., 2005]. Note that the modeled locked and transition zones vary along strike, following the trend of the western edge of Siletzia offshore of central and northern Oregon. The abrupt along-strike change in locking in southern Oregon corresponds to the southern end of Siletzia. Major offshore forearc gravity lows and associated basins generally lie near the western edge of Siletzia and overlie the lower part of our locked zone and much of the transition zone [Wells et al., 2003]. The northern change in locking is also paralleled by a northward-widening area of landward to mixed vergence in the outer accretionary wedge [Mackay et al., 1992; Gutscher et al., 2001]. White circles are epicenters of 2004 earthquakes inferred on the plate boundary [Trehu et al., 2008].

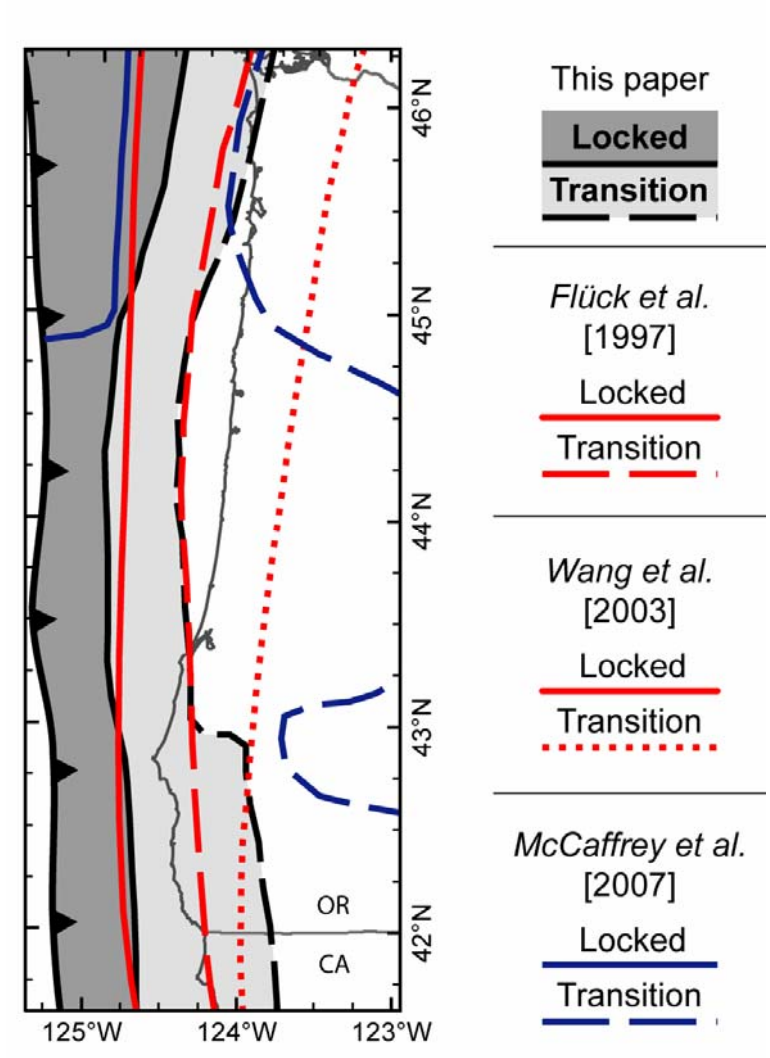

Figure 5. Comparison of locking models for Oregon portion of Cascadia inferred from elastic half-space dislocation modeling using 3-D geometry of the Cascadia megathrust. Solid lines indicate the lower limits of complete locking and the dashed lines indicate the downdip limits of the transition zones (zero contour of slip rate deficit). All models use different parameterizations, such as the convergence rate and the functional form of the downdip slip deficit profile, when solving for the locking distribution. Models constrained with uplift rate data [this paper and Flück et al., 1997] generally have narrower transition zones than those constrained primarily by horizontal deformation data [Wang et al., 2003; McCaffrey et al., 2007].

Part 2: Establishing new tide gauges and leveling lines

Based on the analysis of the regional NGS and NOAA we have chosen several small regions in which we have generated new tidal data, and leveling, and have experimented with a variety of analysis approaches. Figure 6 show the regions we are currently working, and Figures 8-10 show some of our results. In the Siuslaw region (Figure 7) we have re-leveled benchmarks (Figure 8) and installed tide gauges (Figures 7, 8) to continue historic time series to create a

dense EW profile of uplift across the subduction interface. We chose to start with the Siuslaw system to demonstrate the methodology in a convenient location (close to the University of Oregon), and to generate a new EW profile of uplift where in the past there has been none. We are now in the process of applying this methodology to a number of sites along the Pacific NW coast that will greatly improve the accuracy and precision of our regional uplift map, and thus allow more insightful comparisons between GPS and other systems for measuring uplift.

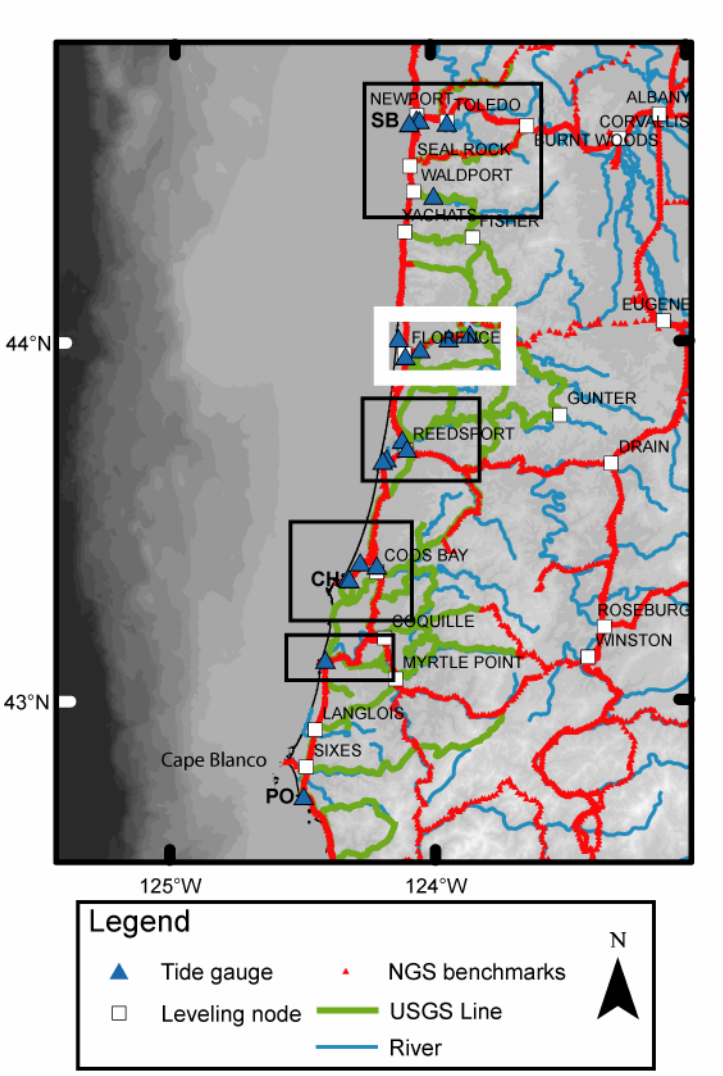

Figure 6. Western Oregon offshore to trench from Cape Blanco to Newport, showing distribution of vertical geodetic datasets. Shaded relief basemap is 250 m DEM (Haugerud, 2000) contoured with 250 m interval. Red lines are NGS first and second order survey lines. The N-S coastal line, Newport-Albany, Reedsport-Drain, and Coquille-Winston were analyzed in previous studies (Mitchell et al., 1994; Hyndman and Wang, 1995). Green lines are historic USGS leveling lines that have not been previously analyzed. The three currently operating tidal stations, South Beach, Charleston, and Port Orford are labeled. Other tidal sites with promising records are shown as blue triangles. White box shows Siuslaw area (Figure 7) below. The black boxes delineate the other

areas where we are constructing detailed E-W profiles of uplift rate in the manner depicted for the Siuslaw area below.

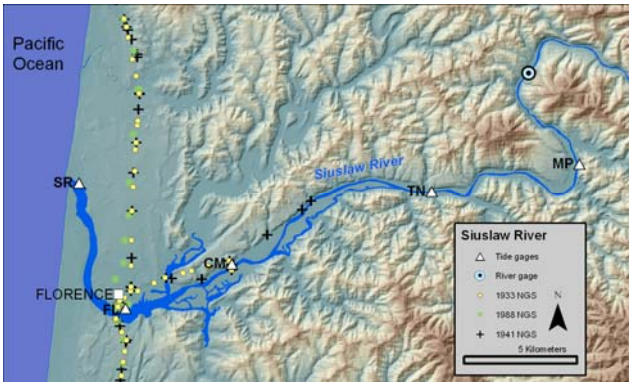

Figure 7. Map of the Siuslaw River estuary showing the five tide gages operated by NOAA in 1974, forming a ~20 km long E-W profile. The Florence site was also occupied for 1 year 1933-34. We have reoccupied all five sites in the summer and fall, 2005. The estuary is tidally controlled from upstream of the town of Mapleton. Repeated National Geodetic Survey work on North-South and East-West transects in the area provides additional geodetic control.

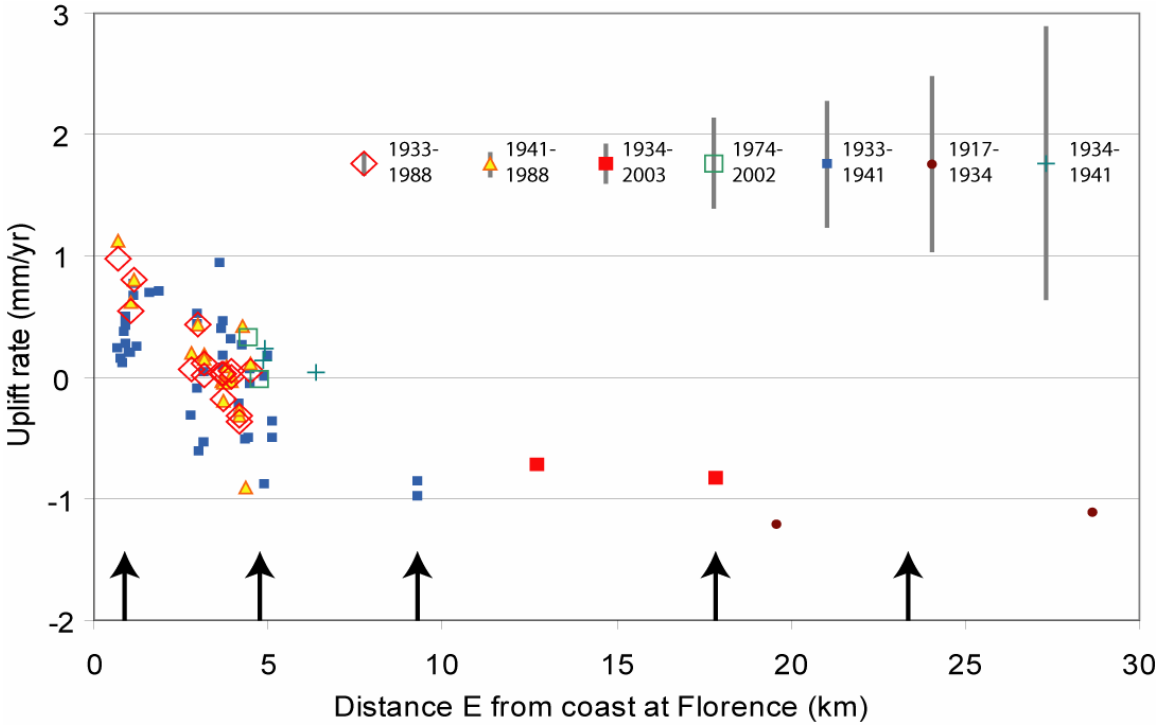

Figure 8. Uplift rate profile along the Siuslaw River from Florence to Mapleton (Figure 7), adjusted to zero uplift at Florence assuming a regional sea level rise rate of 2 mm/yr. Black arrows show the positions of historic tidal observations along the traverse. Leveling data include NGS, USGS, and recent U of Oregon surveying (2002, 2003). The data (including some along the north-south coastal route) have been projected onto an east-west profile line, which is responsible for some of the scatter, particularly on the western end. Representative error bars are portrayed in the legend, based on the total traverse length (29 km), survey order, the interval between observations, and loop closure of multiply-run lines. Note the rapid increase in uplift rate west from Florence.

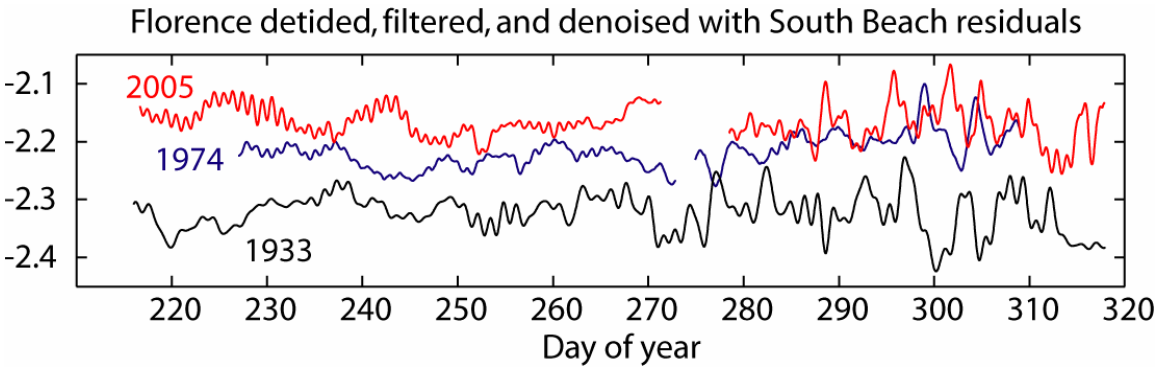

Figure 9. Completely processed water level observations at Florence. There are 3 epochs of sea level observations at Florence: a year in 1933-4, about 3 months in the summer of 1974 and our occupation in the summer of 2005. Because of the strong seasonal differences we only compare the 3 summers (shown here) that have overlapping data. 1974 and 1933 have hourly observations, and 2005 6 minute observations. Note the highly periodic daily cycle seen especially in the early summer portion of the 2005 data. This appears to be due to a highly periodic daily onshore/offshore flow pattern that does not occur as strongly later in the record. Because the impact of this pattern is very different from site to site and through time at each site, we have not yet developed an efficient method for removing it. Also note that all records become much noisier as Winter approaches and the ocean becomes much more variable in height. We have used the South Beach "ocean noise" model on all three series. Because the noise model is the deviation of the South Beach record from a straight line through the South Beach record (Figure 1), the rate of sea level rise at South Beach (the slope of a line through the South Beach data), has little effect on the rate of sea level rise at Florence.

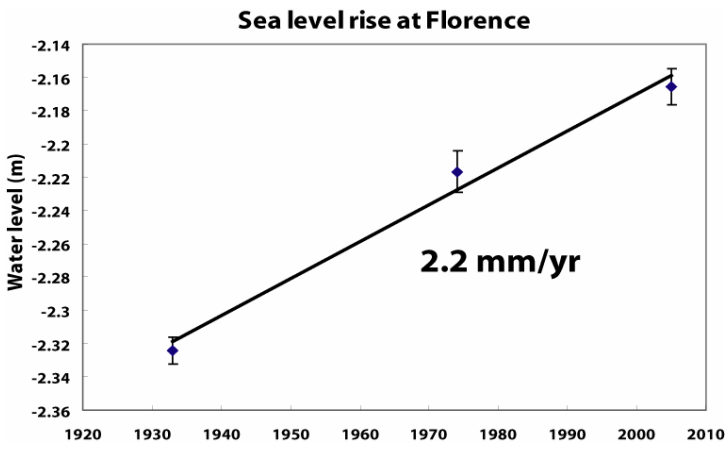

Figure 10. Sea level rise at Florence. Plotting water level means at Florence (from Figure 9) yields a 2.2 mm/yr rate of sea level rise. The values with 2 standard error bars, calculated with an order 10 autoregressive model, are derived from the ~100 day summer period of overlapping records. We have an additional ~300 days from 1933-4 and continue to collect data at Florence so within a year should have a year long comparison between 1933-4 and 2005-6 and one more summer epoch (2006). Given a global sea level rise of ~2 mm/yr, we can conclude that there is essentially no uplift occurring at Florence.

Publications:

Burgette, R. J., Weldon, R. J., Schmidt, D. A., 2008, Interseismic uplift rates for western Oregon and along-strike variation in locking on the Cascadia subduction zone, *Journal of Geophysical Research*, in revision.

Burgette, R. J., 2008, Uplift in response to tectonic convergence: the Kyrgyz Tien Shan and Cascadia subduction zone, Ph.D., University of Oregon, Eugene, OR

Burgette, R. J., Weldon, R. J., Schmidt, D. A., 2007, A more accurate vertical velocity field for coastal Oregon reveals variations in extent of locking on the Cascadia subduction zone: Eos, Transactions, AGU, v. 88, no. 52, Fall Meeting Supplement, Abstract G52A-01.

Weldon, R. J., Burgette, R. J., Schmidt, D. A., 2006, Along-strike variation in locking on the Cascadia subduction zone, Oregon and northern California: Eos, Transactions, AGU, v. 87 no. 52, Fall Meeting Supplement, Abstract T41A-1556.

Burgette, R.J., Weldon, R. J., Livelybrooks, D., Schmidt, D. A., Alba, S. K., and Wisely, B. A., 2005, Constraints on the extent of subduction zone locking along the central Oregon coast from leveling and sea level observations: Eos, Transactions, AGU, v. 86, no. 52, Fall Meeting Supplement, Abstract S51C-1017.